

A First Look at White Dwarf - M Dwarf Pairs in the Sloan Digital Sky Survey (SDSS)

Sean N. Raymond^{1,2}, Paula Szkody², Suzanne L. Hawley², Scott F. Anderson², J. Brinkman³, Kevin R. Covey², P. M. McGehee⁴, D. P. Schneider⁵, Andrew A. West², D. G. York⁶

ABSTRACT

We have identified 109 White Dwarf (WD) - M dwarf pairs in the Sloan Digital Sky Survey (SDSS) with $g < 20$ th magnitude. For each system we determined the temperature of the WD primary and the spectral type of the M dwarf secondary. Using H α emission as a proxy for the chromospheric activity level of the M dwarf, we investigated correlations between the activity level and properties of the system. Compared with field M dwarfs (Hawley et al. 1996), we see a slightly higher active fraction of early-type stars, with activity levels similar to the field.

We have conducted followup observations at the ARC 3.5m telescope to obtain radial velocity information and to search for short period binaries, which may be on the verge of interacting. We report on one system with a 4.1 hour period, and several additional systems with significant velocity variations.

keywords: binaries: spectroscopic — Sloan Digital Sky Survey (SDSS) — stars: activity — stars: late-type — white dwarfs

1. Introduction

The formation and evolution of a low mass star in a binary system is a common phenomenon, and can lead to interesting results such as cataclysmic variables (Warner 1995), which are the most numerous UV and X-ray sources in the Galaxy, and Type Ia supernovae (Langer et al 2000), which are standard candles for cosmology. While the low mass secondaries play a pivotal role in determining the evolution of the system, it is not well understood how the binary environment affects the evolution and properties of the secondary.

¹Corresponding Author: raymond@astro.washington.edu

²Department of Astronomy, University of Washington, Box 351580, Seattle, WA 98195

³Apache Point Observatory, P.O. Box 59, Sunspot, NM 88349-0059

⁴Los Alamos National Laboratory, Los Alamos, NM 87545

⁵Dept. of Astronomy and Astrophysics, The Pennsylvania State University, University Park, PA 16802

⁶Dept. of Astronomy and Astrophysics and Enrico Fermi Institute, 5640 S. Ellis Ave, Chicago, IL 60637

Studies of pre-cataclysmic variable stars (or Pre-Cataclysmic Binaries – PCBs) (Bond et al 1985; Hillwig et al 2000) envision the following scenario for their evolution. The more massive primary in a wide binary star system evolves through the giant and planetary nebula phases, leading to significant mass loss and a “common envelope” encompassing both primary and secondary. A large amount of the system’s orbital angular momentum is lost during this phase, leading to a much closer binary orbit. Tidal interactions in the binary system will have led to synchronous rotation of the secondary for separations closer than 5-7 R_g , where R_g is the radius of the primary during its giant phase (Soker 2002), corresponding to an orbital period of ~ 50 days (assuming an M5 secondary). The remaining binary may undergo further orbital decay via magnetic braking or gravitational radiation (see Warner 1995). Eventually, systems with very short periods will interact and become cataclysmic variables (CVs). CVs therefore represent only the short-period subset of all these binaries. In this paper we add to the growing database of PCBs, focusing on faint WD/M pairs. We hope to eventually build a large sample of PCBs which represents various phases of binary evolution, in order to test the validity of the above scenario, and the efficiency of the various physical mechanisms for angular momentum loss.

Note that we define the WD, the original high-mass component, as the primary in these systems. This contrasts with previous surveys, many of which defined the primary as the brighter star in a given filter, whether it be the WD or the M dwarf.

The Sloan Digital Sky Survey (SDSS; York et al 2000) database, with its accurate photometry in five broad bands covering the entire optical spectrum, is an outstanding resource for finding these pre-interacting systems. We have identified 109 WD/M binaries with $g < 20$, using data available through 11/14/2001. Our efficiency at finding these objects using our current photometric targeting algorithm is $\sim 60\%$, and our sample is augmented by serendipitous observations obtained through other target selection pipelines (e.g. quasars). Forty three of our systems are contained in the June 2001 SDSS Early Data Release (Stoughton et al 2002).

Currently known are 42 PCBs (Hillwig et al 2000), and roughly 800 widely separated, non-interacting WD/M binaries (Silvestri, Oswald & Hawley 2002 and references therein). We expect to accumulate a sample of 700-1000 systems by the end of the survey, including ~ 50 PCBs – doubling the current samples of these objects.

For each of our systems, we analyzed the SDSS discovery spectrum to determine the temperature and distance of the white dwarf primary and the spectral type and magnetic activity level of the low mass secondary. We are particularly interested in studying the dependence of the magnetic activity level on rotation rate, which increases in close binary systems where the secondary is in synchronous rotation. The magnetic activity of the secondary has been widely cited as a primary driver for angular momentum loss as stars evolve toward the period gap (Patterson 1984). We also investigated the influence of irradiation from the hot white dwarf on the activity level of the secondary.

To further compare activity levels across spectral type and rotation rate, we need to determine

which pairs are in close binaries (thus exhibiting synchronous rotation). Population models (de Kool 1992; Warner 1995 and references therein) indicate that about 10% of the WD/M pairs should be close enough to enter the common envelope stage, with periods ≤ 4 hrs. We targeted the most active systems for followup observations at the 3.5m ARC telescope at Apache Point Observatory (APO), to search for radial velocity variations, and obtain orbital periods. For a $2 M_{\odot}$ WD progenitor, a secondary closer than ~ 0.25 AU ($P \leq 50$ days) will rotate synchronously (Soker 1996). The radial velocity of an M5 dwarf ($M \approx 0.2 M_{\odot}$) in such a binary is $\sim 40 \text{ km s}^{-1}$. With our radial velocity errors of $\pm 10 \text{ km s}^{-1}$, we can therefore detect both synchronously and non-synchronously rotating binaries.

In Section 2 we describe our technique for selecting WD/M pairs from the SDSS photometric database. Section 3 presents our methods for deriving system parameters from the SDSS spectra. In Section 4 we discuss the results of this analysis, including our ongoing followup at APO. Section 5 summarizes our findings.

2. SDSS and APO Data

2.1. Photometric Selection of WD/M Pairs with SDSS

Our goal is to find the evolutionary precursors of CVs, systems on the verge of interacting, or only weakly interacting. For these systems we expect no significant flux from an accretion disk, and the composite spectrum of the candidate pair will be simply the superposition of the spectra of each component. Therefore we wish to isolate objects with blue spectral energy distributions (SEDs) at short optical wavelengths (hot WDs), and red SEDs at long wavelengths (M dwarfs). To accomplish this, we use the Sloan filter system (Fukugita et al 1996) to devise a photometric targeting algorithm.

Through a trial and error procedure during the commissioning year of the SDSS, we optimized a set of color selection criteria in the 4 SDSS colors: $u - g < 0.45$ (blue), $g - r < 0.7$ (blue), $r - i > 0.3$ (red), and $i - z > 0.4$ (red). We found that a practical magnitude cutoff of $g < 20$ was required to obtain targeted SDSS spectra of our candidates with a sufficient signal to noise ratio for subsequent analysis.

Figure 1 shows the color distribution of our full sample of 109 systems. About half of the sample was found by visual inspection of SDSS spectra targeted for other purposes (e.g. galaxies, quasars), and many of these objects lie outside of our color cuts. However, we are unable to broaden the color selection criteria further, as too many interlopers from the stellar locus would be targeted, lowering our efficiency.

When our color criteria are applied to all SDSS objects for which spectra have been taken, $\sim 60\%$ of these are WD/M pairs. We have repeat observations of 16 systems, one of which was observed 3 times. Note that our sample is not at all complete, as we take an average of one spectrum

per SDSS field, which is 7 square degrees. The completeness of and biases in our sample will be addressed in an upcoming paper based on a larger SDSS WD/M sample.

Table 1 lists the SDSS photometry for the full sample, and Figure 2 illustrates the wide variety of systems we observed. Panels a) and b) are classic WD/M pairs, with SEDs that are blue at short wavelengths and red at long wavelengths. In some cases, the binary spectrum is dominated by the hot WD primary (panel c) or the cool M dwarf secondary (panels d and f), while panel e) shows nearly equal contributions over the whole spectrum. Panels a) and c) show very active systems with strong $H\alpha$ emission and emission cores inside the pressure-broadened WD Balmer absorption lines. The WD primaries in the systems from panels d) and f) are similar, however, d) is active while f) is not.

2.2. APO Data

We have observed 31 of our 109 pairs with the ARC 3.5-m telescope at APO, using the high resolution grating on the Double Imaging Spectrograph (DIS), which produces spectra in both the blue and red portions of the optical spectrum simultaneously. The dispersion is about 1.6\AA pixel^{-1} in the blue, and 1.1\AA pixel^{-1} in the red.

Table 3 shows information for the 12 systems with APO spectra on at least two different nights. We tracked 5 objects for several hours, to look for variations on ≤ 4 hour timescales.

3. Analysis of SDSS Data

The temperature of the WD primary in each spectrum was determined by fitting the spectrum to hydrogen WD models (Hubeny & Lanz, 1995). Only one object, SDSS144258.48+001031.5, showed helium absorption lines. We fit the spectra between 3800 and 5000 \AA , a region with very little contamination from the M dwarf secondary, to models with temperatures between 8,000K and 98,000K. The models are normalized to the spectrum at 4200 \AA , which is a fairly flat region of continuum between the strong $H\delta$ and $H\gamma$ absorption lines. The best fit was found using a simple chi-squared minimization technique. The errors are, conservatively, $\pm 2,000\text{K}$ for temperatures below 20,000K, and $\pm 4,000\text{K}$ above 20,000K. Once the best fit temperature was determined, the distance was found from the normalization factor that matches the model flux to the spectrum, assuming a WD radius of 8×10^8 cm ($M_{WD} = 0.6 M_{\odot}$). We then subtracted the best-fit WD model from the binary spectrum to extract the spectrum of the low mass secondary.

The spectral types of the secondaries were determined from these extracted spectra, using primarily the TiO5 spectral index defined in Reid, Hawley and Gizis (1995). This index measures the strong TiO band near 7050 \AA , and is well correlated with spectral type over the range K7 - M6. There are no secondaries with later types in our sample, which is expected given the extreme

faintness of these very late M dwarfs (precluding their selection in our sample).

The distances obtained from the WD analysis were checked using the spectroscopic parallaxes of the M dwarf secondaries. We obtained absolute magnitudes for the M dwarfs as a function of spectral type using relations from Hawley et al (2002). The distances from the two methods generally agreed within 20%. However, the spectroscopic parallax of late-type stars using SDSS colors is under revision (West et al in preparation). We therefore use the distances derived from the WD temperature fitting.

The activity level of an M star is best measured by the ratio of its $H\alpha$ luminosity to its bolometric luminosity, $L_{H\alpha}/L_{bol}$. The $H\alpha$ equivalent width (EW) of each star was measured interactively using the IRAF “splot” routine, as continuum placement is difficult in these subtracted spectra, making automatic routines unreliable. The $H\alpha$ luminosities of our M dwarfs were calculated from the equivalent widths using the average $H\alpha$ continuum fluxes as a function of spectral type from the PMSU sample (Hawley, Gizis & Reid 1996). The bolometric luminosities were calculated from the spectral type averages given in Reid and Hawley 2000 (*New Light on Dark Stars*). Table 1 contains all of the WD and M dwarf parameters determined from our analysis. Table 2 bins the data by the spectral type of the secondary.

4. Results

Figure 3 shows the temperature distribution of the white dwarfs in our sample. The average temperature is $\sim 16,000\text{K}$, slightly higher than the average for field WDs, which is $\sim 12,000\text{K}$. The highest temperature seen is $\sim 44,000\text{K} \pm 4,000\text{K}$. Thus, using the cooling curves from Fontaine et al (2001) and assuming a mass of $0.6 M_{\odot}$, the youngest (hottest) WD has a post main-sequence age of less than 0.1 Gyr. The coolest model was $8,000\text{K}$, implying a post main-sequence age between 1 and 2 Gyr.

The average M spectral type of the low mass secondaries is $\sim \text{M4.5}$. The distribution of spectral types of the sample is shown in Figure 4. The rise toward spectral type M4-5 is due to the mass function of the local neighborhood, while the decrease toward later spectral types is due to the lower detection efficiency for fainter objects.

The distribution of derived distances is shown in Figure 5, assuming radii of 8×10^8 cm for all WDs, which should be a valid assumption for at least $\sim 80\%$ of WDs (Bergeron et al 1992). All but one of the systems lie within 200 pc, indicating that we are sampling the local disk population.

Roughly 60% of the systems are magnetically active (see Table 2). This is a higher fraction for these early-mid M dwarfs than that measured by the Palomar/MSU (PMSU) Survey of nearby stars (Hawley, Gizis & Reid 1996). As noted in the PMSU Survey and for later types by Gizis et al (2000), the fraction of stars that are active increases with later spectral type, until virtually every M7 star is active. Figure 6 shows that a higher fraction of early-type M dwarf components (M1 -

M4) in WD/M pairs are active than their field counterparts. The level of activity as measured by $L_{H\alpha}/L_{bol}$ (Figure 7) is similar for active M dwarfs both in the field and in our binaries, but there is a possible suggestion that the M2 - M4 dwarfs in the WD/M pairs are somewhat more active. However, our sample is relatively small, with few points earlier than M2.5 or later than M6, so these results must be confirmed by further studies with a larger sample.

Surprisingly, Figure 8 shows only a very weak correlation between M dwarf activity and WD temperature. A stronger correlation would imply that irradiation by the WD was enhancing the $H\alpha$ emission from the M dwarf.

The source of magnetic activity in late type stars is not well understood, and information on the rotation dependence of the activity would provide a constraint on existing dynamo models. Close binaries, with large radial velocity variations, should have strong enough tidal effects to induce the M dwarf secondary to rotate synchronously with the white dwarf primary, thereby significantly increasing its rotation rate. If the M dwarf dynamo is rotation dependent, the activity level should thus increase in these close binary systems.

For the 12 objects with at least two followup APO spectra, we can calculate a lower limit for the radial velocity variation. Figure 9 compares their activity levels with V_{min} (i.e. their minimum $v \sin i$). No correlation is immediately apparent, but again more data are needed to provide a significant test. One object out of the five that we tracked for 3 continuous hours, SDSS112909.50+663704.4, was found to have a period of ~ 4.1 hours (see Figure 10). No clear periodicity was found in the four other systems.

5. Conclusions

We have compiled a sample of 109 WD/M binaries from the first year of the Sloan Digital Sky Survey. We expect the sample to contain 700-1000 systems by the end of the five year survey. These systems, which are the precursors of cataclysmic variable stars and type Ia supernovae, span a wide range in WD temperature, M dwarf spectral type and chromospheric activity level.

The average temperature of our sample is $\sim 16,000\text{K}$, considerably hotter than the average temperature for field WDs. The mean spectral class of the low-mass secondaries is $\sim \text{M4-M5}$. The fraction of active early-type M dwarfs in binaries appears higher than the active fraction among field M dwarfs (Figure 6). Their magnetic activity levels may also be elevated relative to those seen in the field M dwarfs (Figure 7). More data are required to confirm and quantify these suggestive results.

Since a higher orbital velocity implies a closer orbit, in which tidal interactions spin up the M dwarf secondary and possibly increase the efficiency of a rotation-dependent dynamo, we have begun to obtain orbital velocities for the brightest, most active systems in our sample.

Population models (de Kool 1992) predict that $\sim 10\%$ of WD/M binaries should be pre-

interacting with orbital periods of ~ 4 hours. We have discovered one such system from the five which were followed for 3 or more hours. Eleven other systems show some evidence for velocity variations during scattered observations. We see no correlation between the minimum orbital velocity and the M dwarf activity level. However, much more data are needed to reach any firm conclusions. Our sample size is continuously increasing, and further analysis and followup observations are in progress. We encourage others to pursue velocities of the identified systems.

Funding for the creation and distribution of the SDSS Archive has been provided by the Alfred P. Sloan Foundation, the Participating Institutions, the National Aeronautics and Space Administration, the National Science Foundation, the U.S. Department of Energy, the Japanese Monbukagakusho, and the Max Planck Society. The SDSS Web site is <http://www.sdss.org/>.

The SDSS is managed by the Astrophysical Research Consortium (ARC) for the Participating Institutions. The Participating Institutions are The University of Chicago, Fermilab, the Institute for Advanced Study, the Japan Participation Group, The Johns Hopkins University, Los Alamos National Laboratory, the Max-Planck-Institute for Astronomy (MPIA), the Max-Planck-Institute for Astrophysics (MPA), New Mexico State University, University of Pittsburgh, Princeton University, the United States Naval Observatory, and the University of Washington.

REFERENCES

- Bergeron et al. 1992, ApJ, 394, 228
- Blanton, M.R., Lupton, R.H., Maley, F.M., Young, N., Zehavi, I., & Loveday, J. 2002, AJ, submitted
- Bond, H. E., Cataclysmic Variables and low-mass X-ray binaries; Proceedings of the Seventh North American Workshop, Cambridge, MA, January 12-15, 1983 (A85-48276 23-90). Dordrecht, D. Reidel Publishing Co., 1985, p. 15-27.
- Fan, X. 1999, AJ, 117, 2528
- Fontaine, G. Brassard, P., & Bergeron, P., 2001, PASP, 113, 409
- Fukugita, M., Ichikawa, T., Gunn, J. E., Doi, M., Shimasaku, K. & Schneider, D. P. 1996, AJ, 111, 1748
- Gizis, J. E. et al. 2001, AJ, 120, 1085
- Gizis, J. E., Reid, I. N. & Hawley, S. L. AJ123, 3356
- Gunn, J. E. et al. 1998, AJ, 116, 3040
- Hawley, S. L., Gizis, J. E. & Reid, I. N. 1996, AJ, 112, 2799
- Hillwig, Todd C., Honeycutt, R. Kent, & Robertson, Jeff W., 2000, AJ, 120, 1113
- Hogg, D.W., Finkbeiner, D.P., Schlegel, D.J., & Gunn, J.E. 2001, AJ, 122, 2129
- Hubeny, I. & Lanz, T. 1995, ApJ, 439, 875

- Kirkpatrick, J. D., Henry, Todd J., McCarthy, & Donald W., Jr. 1991, ApJ Supplement Series, 77, 417
- de Kool, M. 1992, A&A, 261, 188
- Langer, N., Deutschmann, A., Wellstein, S., & Hofflich, P., 2000, Astronomy & Astrophysics, 362, 1046-1064
- Lupton, R. H., Gunn, J. E. & Szalay, A. 1999, AJ, 118, 1406
- Lupton, R. H., Gunn, J. E., Ivezić, Z., Knapp, G. R., Kent, S. M. & Yasuda, N. 2002, ASP Conf. Ser. 238, in press (astro-ph/0101420)
- Patterson, J. 1984, ApJ Suppl, 54, 443.
- Pier, J.R., et al 2002 AJ, submitted
- Raymond, S., Szkody, P. & Hawley, S. L. 2001, Cool Stars 12 Conf. Proc. in press
- Reid, I. N. & Hawley, S.L. 2000, *New Light on Dark Stars*, Springer–Praxis Publishing
- Silvestri, N. M, Oswalt, T. D., & Hawley, S.L. 2002, AJ, 124, 1118
- Smith, J.A., et al 2002, AJ, 123, 2121
- Soker, N. 1996, ApJ, 460, L53
- Soker, N. 2002, MNRAS, 336, 1229
- Stoughton, C. et al. 2002, AJ, 123, 485
- Szkody, P. et al. 2002, AJ, 123, 430
- Warner, B. in Cataclysmic Variable Stars, 1995, CUP
- West, A. A., Hawley, S. L. et al. 2003, in preparation
- York, D. G. et al. 2000, AJ, 120, 1579

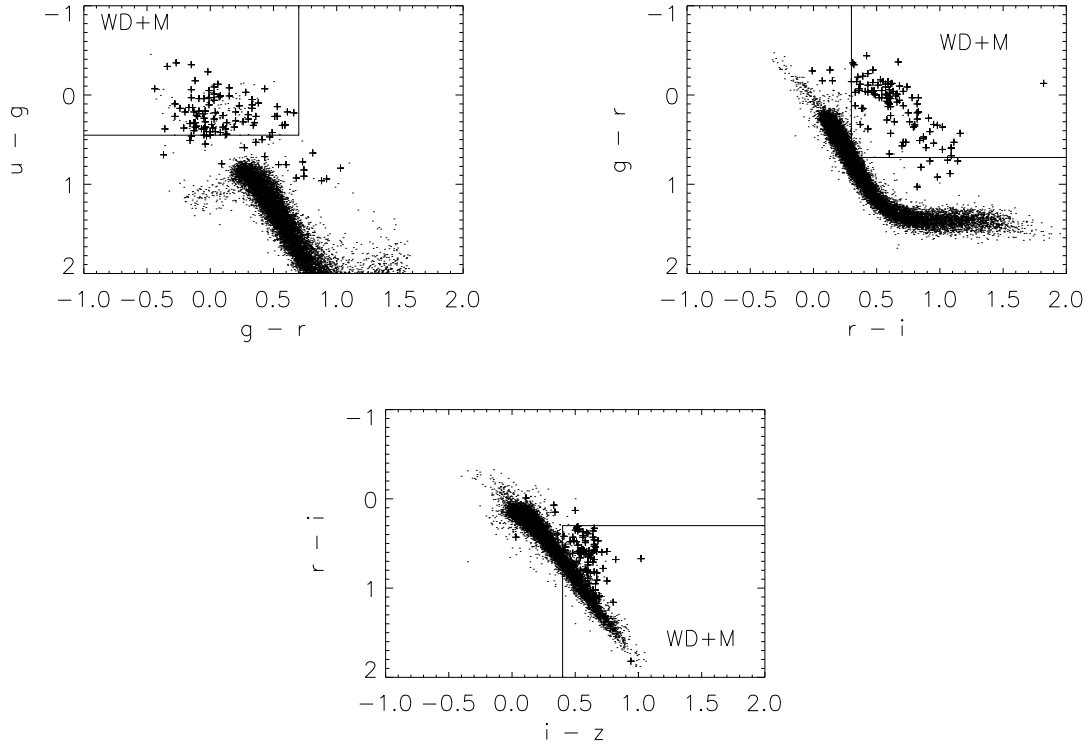


Fig. 1.— SDSS color-color plots of our 109 WD/M pairs. The crosses are the WD/M binaries while the small dots are stars defining the stellar locus. Objects are selected which have blue colors at short wavelengths (hot WDs) and red colors at longer wavelengths (M-dwarfs). Our color criteria are: $u - g < 0.45$, $g - r < 0.7$, $r - i > 0.3$, and $i - z > 0.4$.

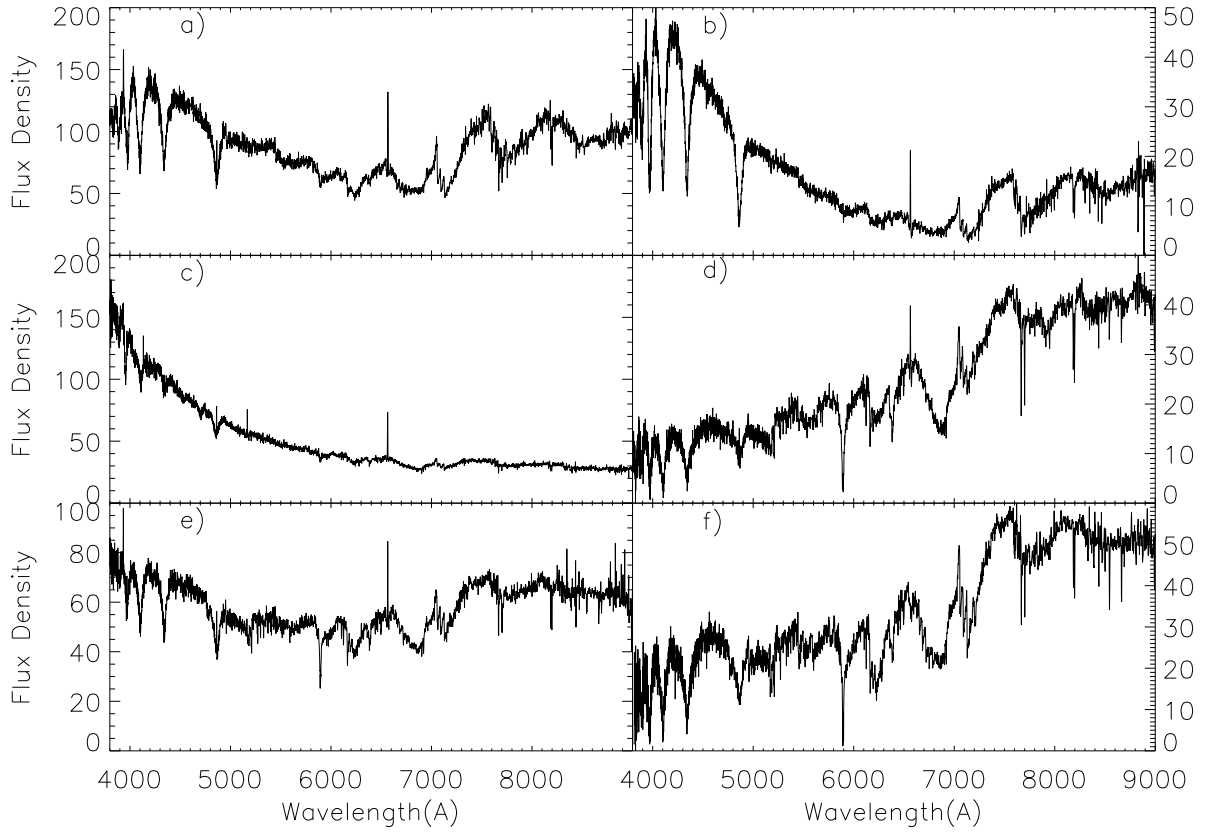


Fig. 2.— Sample of WD/M binary spectra from our sample. Flux density is in units of 10^{-17} ergs cm^{-2} s^{-1} \AA^{-1} . The spectra are: a) SDSS03067.2-003114.4, b) SDSS112909.50+663704.4, c) SDSS001749.25-000955.4, d) SDSS172043.87+560109.3, e) SDSS231230.79+005321.7, and f) SDSS032842.92+001749.8. SDSS112909.50+663704.4 (panel b) has a period of ~ 4.1 hours (see Figure 10).

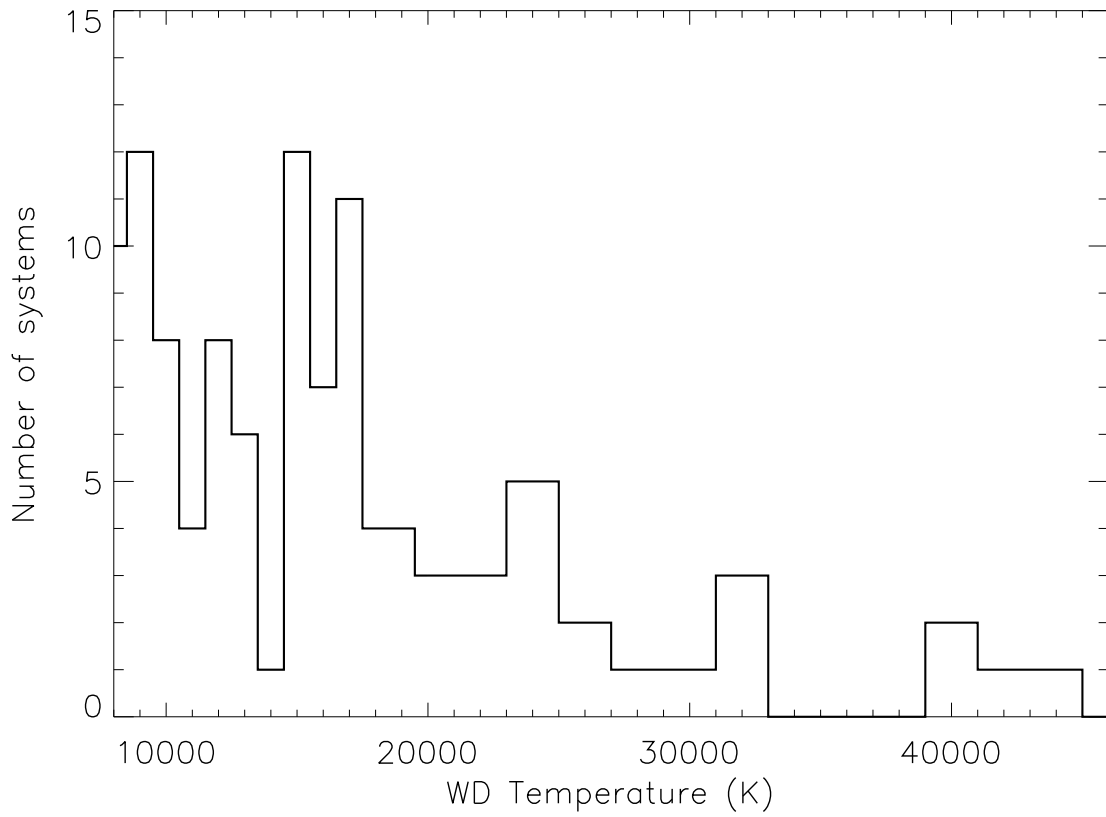


Fig. 3.— Temperature distribution for the 109 white dwarfs in our sample. The average temperature is 16,000K and the hottest is 44,000K. Our coolest WD model had a temperature of 8,000K.

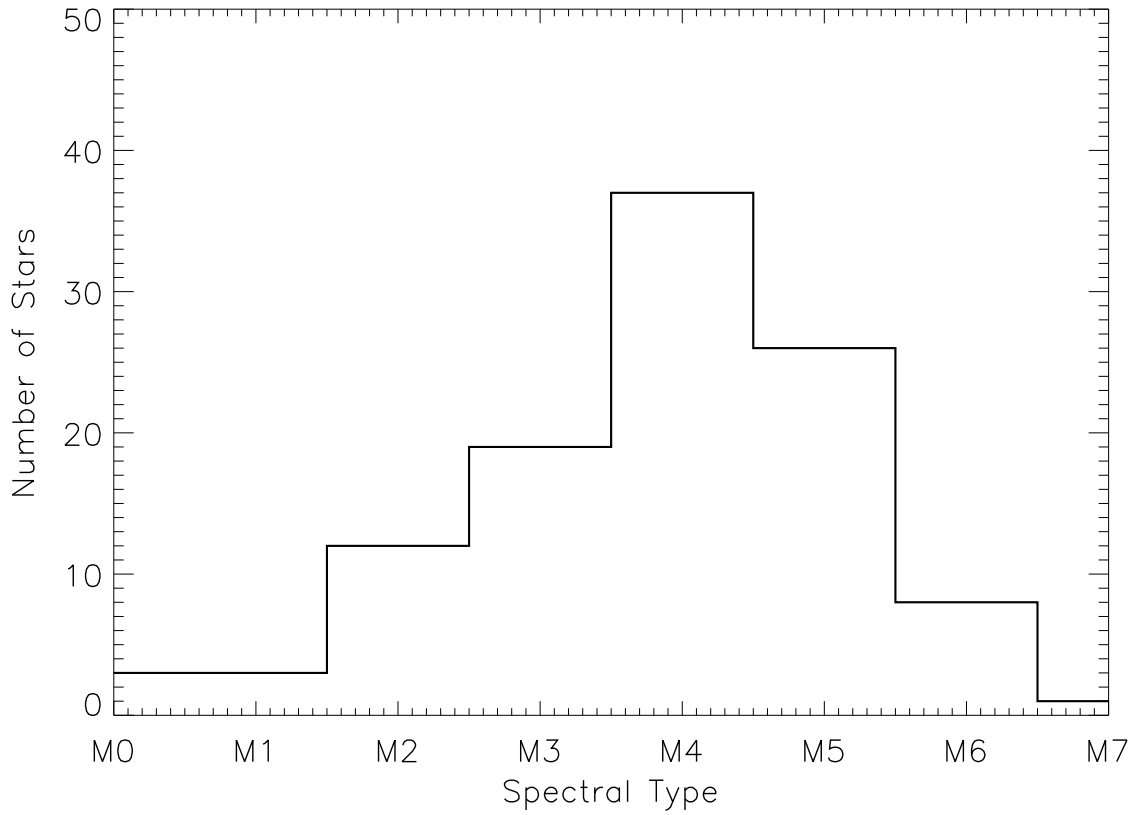


Fig. 4.— Distribution of the M spectral types for our 109 systems, after subtracting off the WDs. The average spectral type is M4.3, and the errors are roughly ± 1 spectral type. The peak at \sim M4.5 is a result of convolving the mass function of the Galactic Disk (which increases for later spectral types) with the detection efficiency (which decreases for later spectral types).

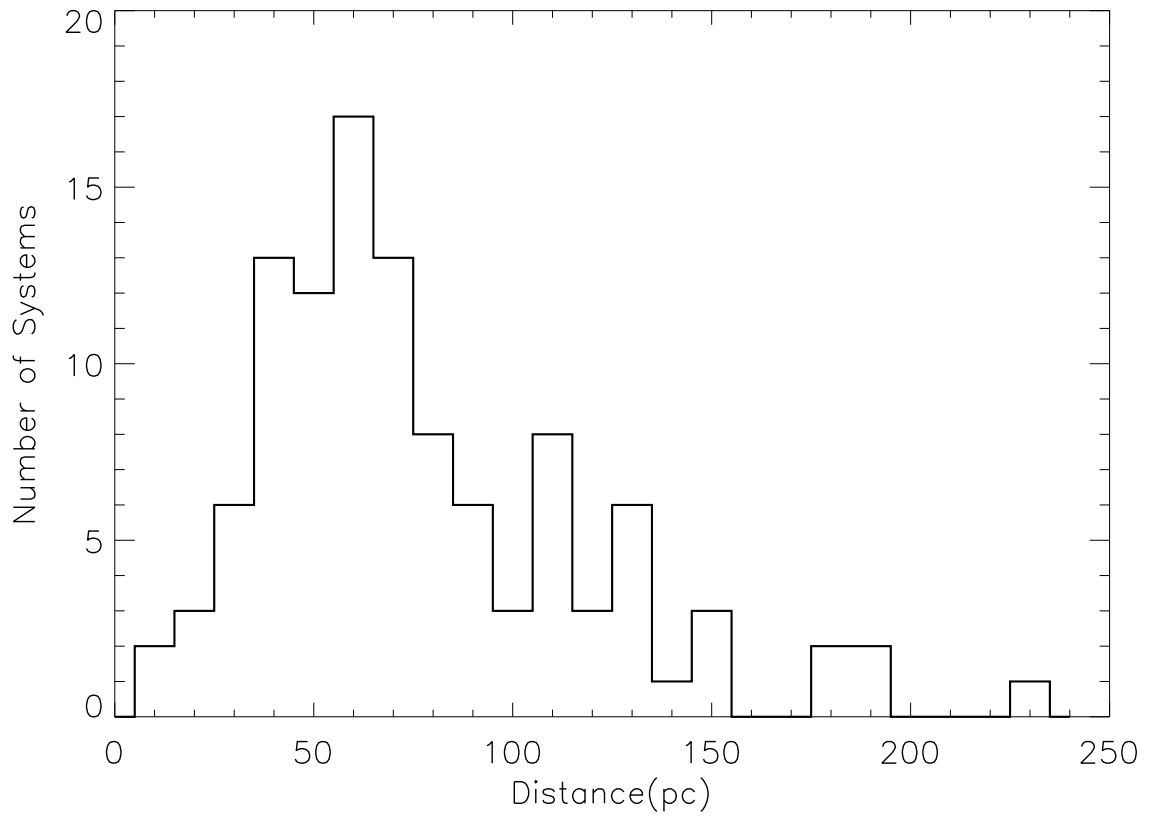


Fig. 5.— Distribution of distances for our 109 systems. These are calculated from the WD model normalization factor, assuming a WD radius of 8×10^8 cm, which is expected for a $0.6 M_{\odot}$ WD. The average distance is 80pc.

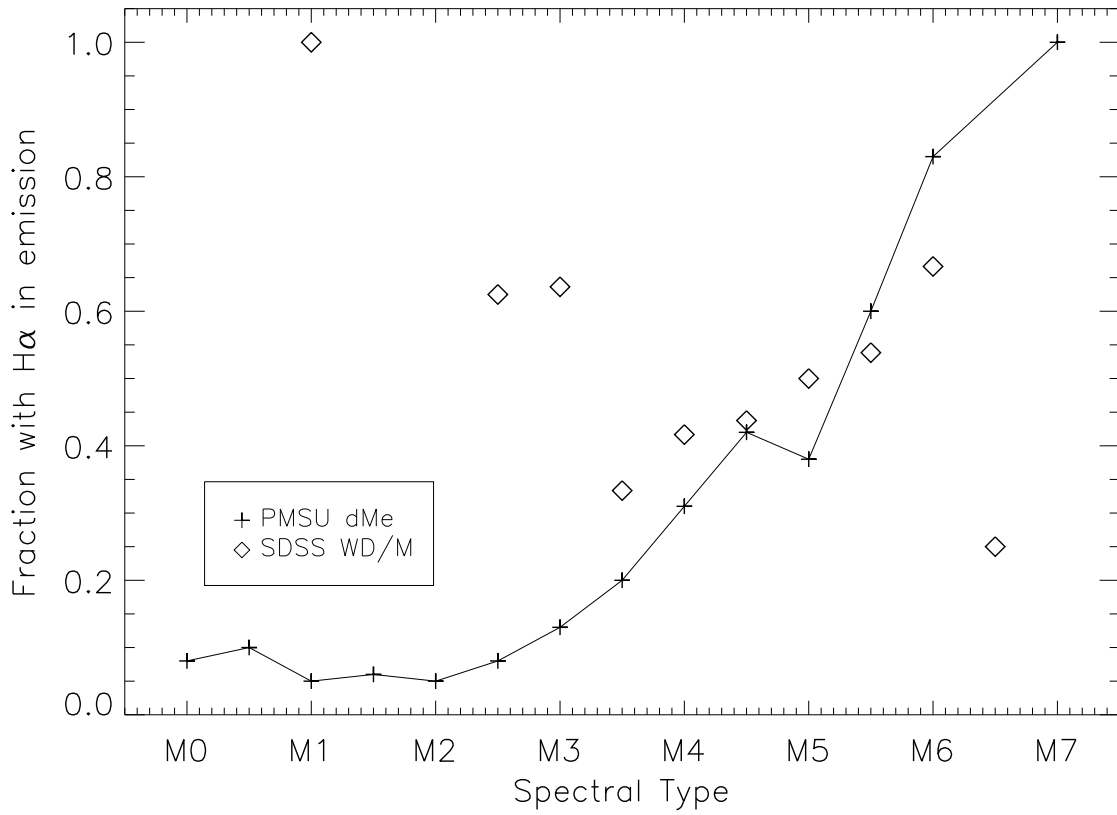


Fig. 6.— Fraction of M dwarfs showing magnetic activity vs spectral type. A higher fraction of the early-type M dwarfs (M1-M4) are active compared with their field counterparts. Table 2 contains the data for Figures 6-8.

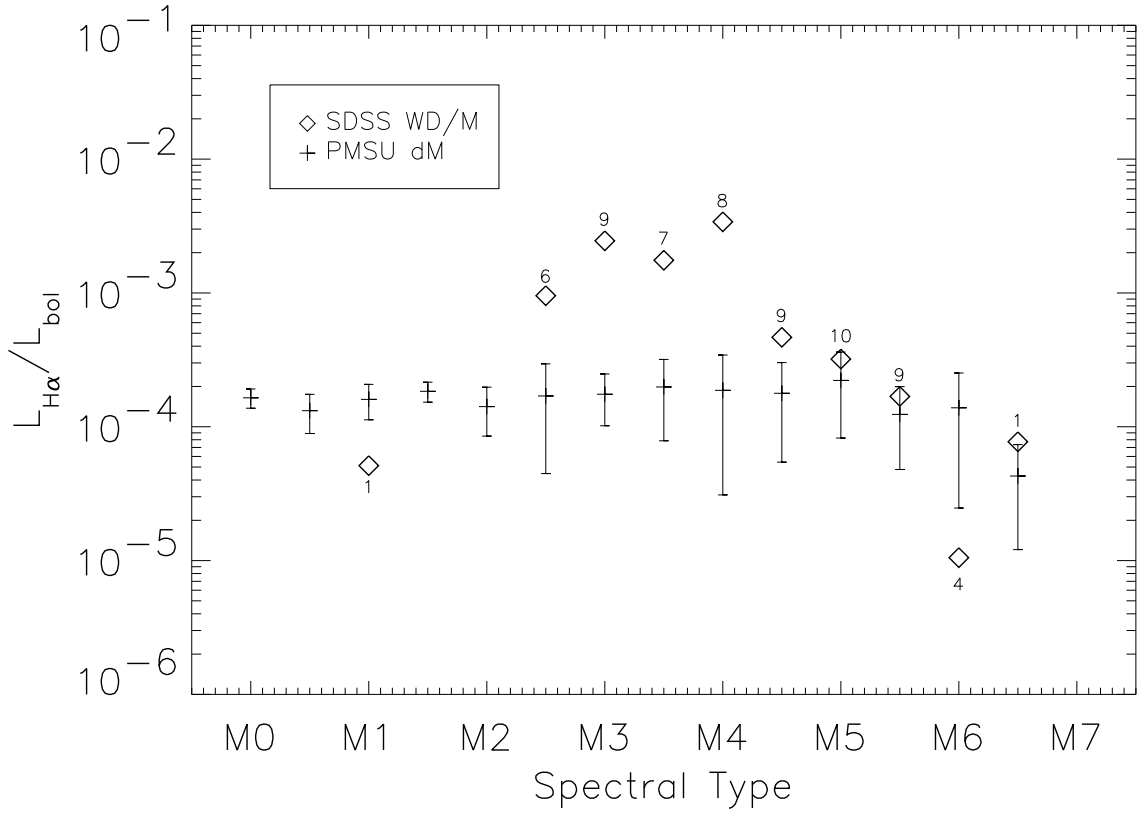


Fig. 7.— M dwarf activity level vs spectral type for the WD/M pairs compared with the PMSU field M dwarfs (Hawley, Gizis & Reid 1996). The numbers near the diamonds indicate how many stars are in each bin. The uncertainties are listed in Table 2. It appears that the M2.5-M4 secondaries have a higher average activity level than their field counterparts, but the number of objects is still too small to make a strong statement.

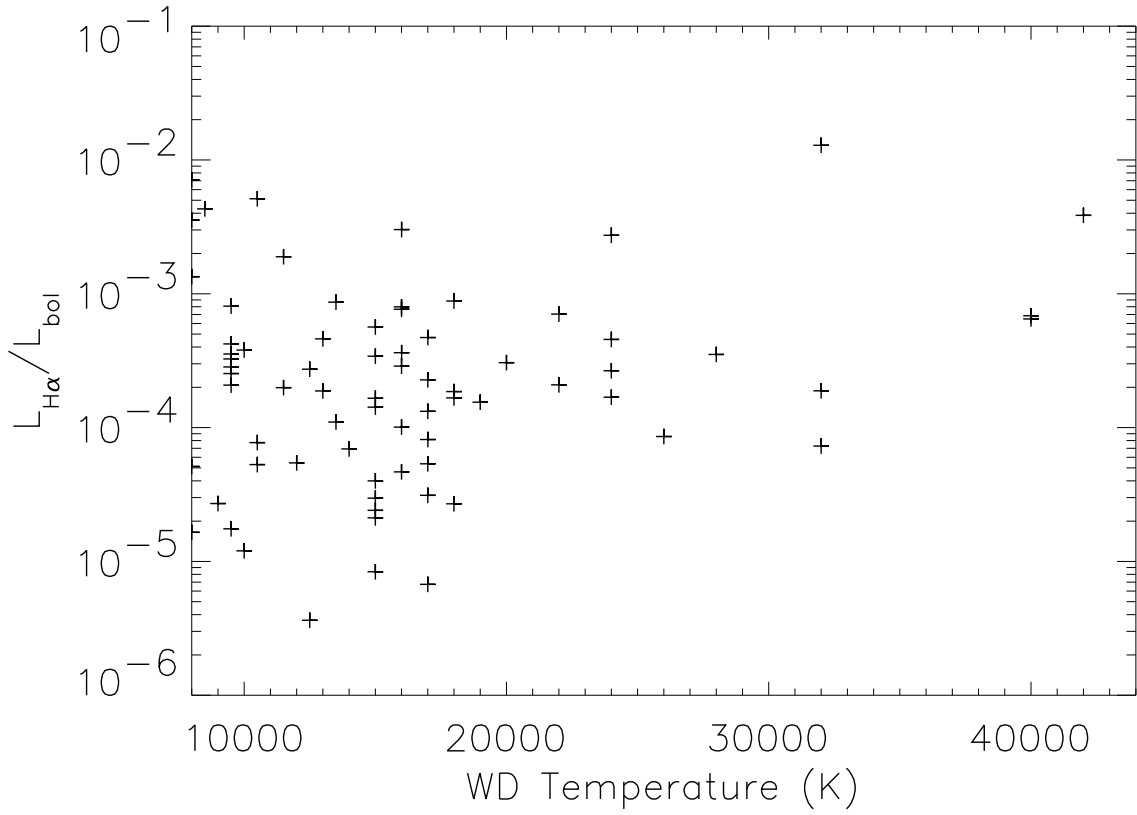


Fig. 8.— M dwarf activity vs WD temperature. The average error bar is 5×10^{-4} . There is a weak correlation between WD temperature and M dwarf activity level, which may be confirmed with a larger sample. There may also be an age-activity effect (Gizis, Reid & Hawley 2002), as older white dwarfs have lower temperatures.

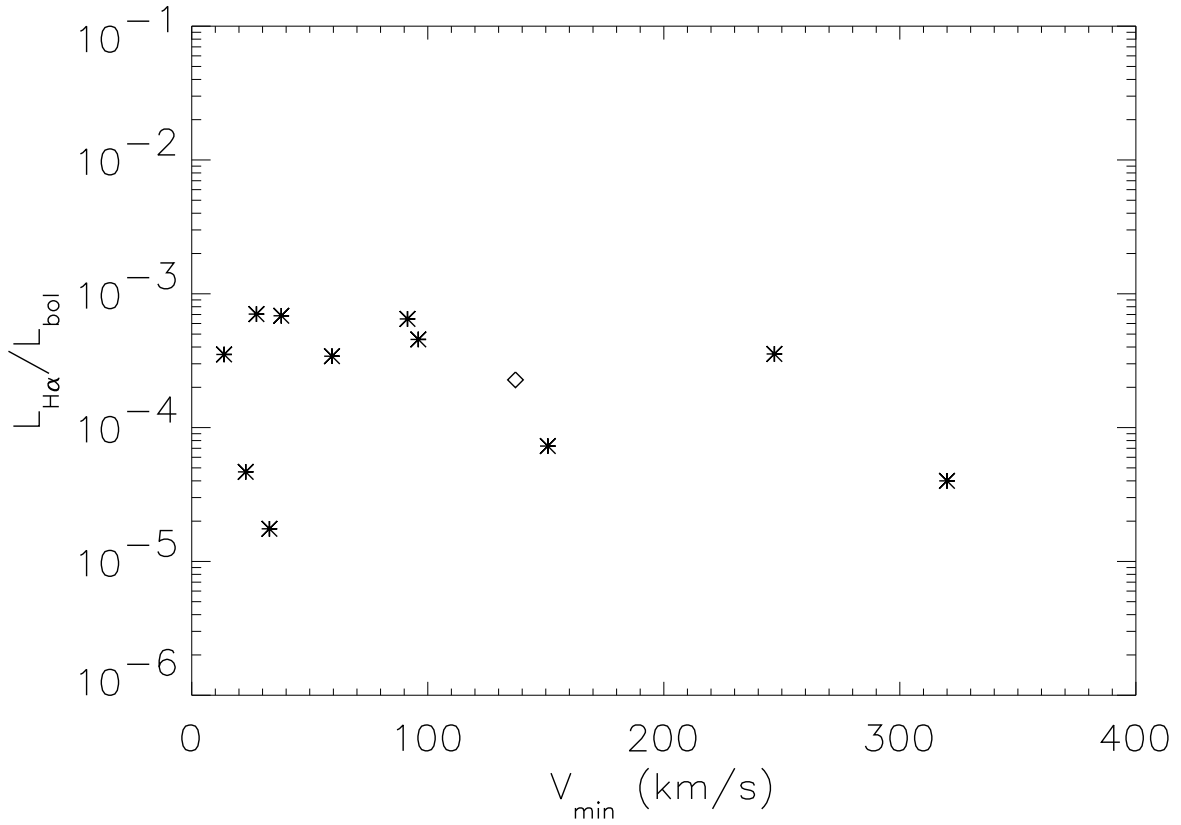


Fig. 9.— Activity level vs V_{min} (minimum $v \sin i$) for the 12 systems in Table 3, based on the observed variation of the H α emission line. SDSS112909.50+663704.4, shown as a diamond, has a 4.1 hour period (see Figure 10). Inclination effects would move points to the right on this plot, i.e. to higher true orbital velocities at the same activity level.

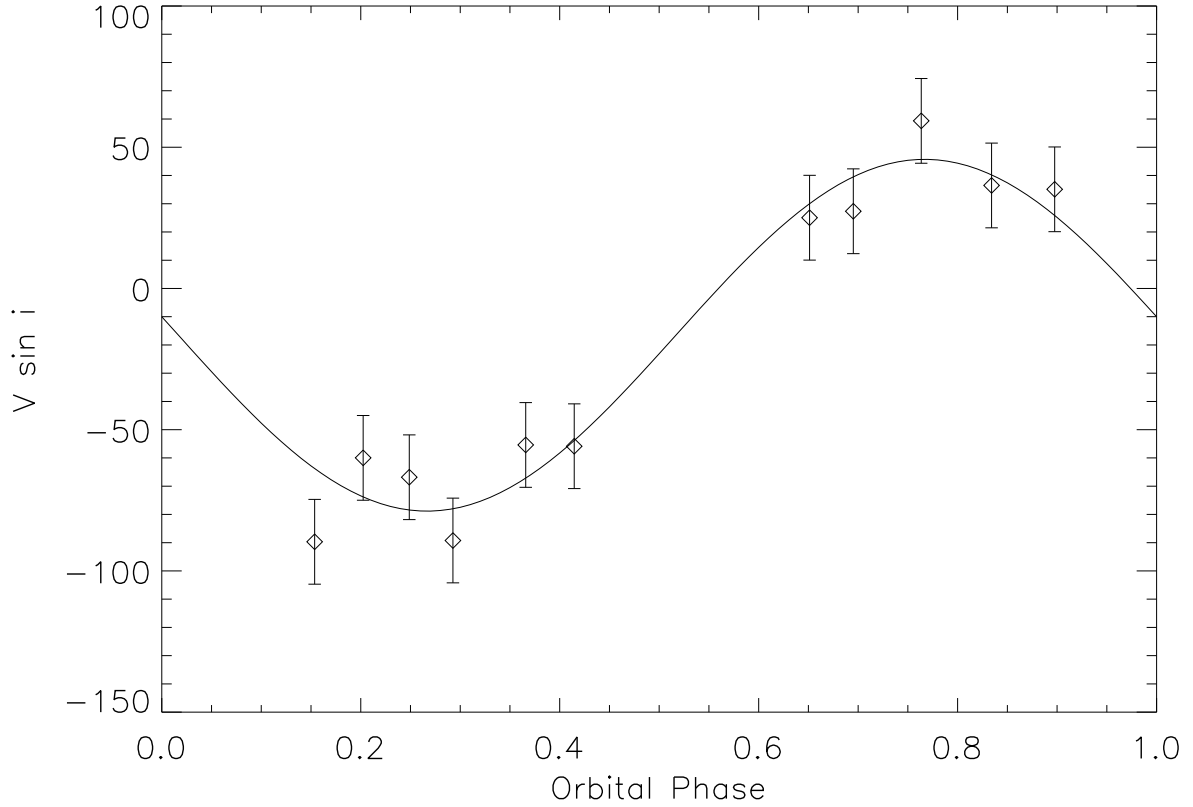


Fig. 10.— Velocity curve for SDSS112909.50+663704.4, showing a 4.1 hour period. The velocities were calculated using the $H\alpha$ emission line. The best-fit parameters are: $P = 4.1 \text{ hrs} \pm 0.1 \text{ hrs}$, $K = 62.3 \text{ km s}^{-1} \pm 4.7 \text{ km s}^{-1}$, $\gamma = -16.6 \text{ km s}^{-1} \pm 0.4 \text{ km s}^{-1}$, and $\phi_0 = 0.017 \pm 0.019$. Assuming a white dwarf mass of $0.6 M_{\odot}$ and an M4.5 mass of $0.2 M_{\odot}$ (Reid & Hawley 2000), this implies a separation of $\sim 10^{11} \text{ cm}$ ($\approx 1.4 R_{\odot}$). This places the system slightly outside the expected region for mass transfer.

Table 1. WD/M Binary Parameters

SDSS J	g	$u-g$	$g-r$	$r-i$	$i-z$	T(WD) ^a	M sp type ^b	d(pc) ^c	EW[H α]
001726.64–002451.2	19.34	0.59	0.27	0.82	0.59	12500	5	87	4.2
001733.59+004030.4 ^g	19.63	0.69	0.43	1.16	0.80	8500	5	57	0.0
001749.25–000955.4 ^{df}	16.88	-0.34	-0.15	0.30	0.28	40000	2	90	8.6
002750.00–001023.4	18.36	0.15	0.33	0.80	0.59	44000	4	193	0.0
005208.42–005134.6 ^g	18.27	0.78	0.60	1.09	0.66	10000	5	42	0.0
005457.61–002517.1 ^g	18.43	0.38	-0.36	0.31	0.52	17000	7	86	3.1
012259.53+154253.8	18.96	0.36	-0.04	0.41	0.56	12500	5.5	75	0.0
012527.14+010255.4	19.82	0.20	0.04	0.59	0.59	24000	3	191	3.0
014152.51–005241.7 ^g	19.76	0.78	0.54	0.95	0.61	8000	5	68	23.0
020351.29+004025.1 ^{dg}	19.35	0.93	0.68	1.09	0.60	9500	3	80	0.0
020806.39+001834.0 ^g	17.25	0.67	-0.37	0.67	1.02	10000	5	20	8.2
021239.46+001856.9	19.41	0.53	0.36	1.02	0.64	17000	4	109	5.2
021411.35+011533.3	19.88	0.65	0.81	0.85	0.46	9000	2.5	63	0.3
021534.78+141846.7	19.55	0.01	0.15	0.39	0.36	24000	3	183	0.0
022835.93–074032.4	18.75	0.36	-0.12	0.37	0.56	15000	5.5	83	0.0
023515.12–000737.0 ^{fg}	16.71	0.24	0.51	0.84	0.54	9500	5	19	2.8
024642.55+004137.2 ^g	19.15	0.84	0.74	1.14	0.63	9500	4	56	8.8
025610.61–073024.6	16.83	0.41	0.00	0.58	0.61	14000	5.5	33	11.0
025622.04–065036.2 ^g	19.45	0.42	0.08	0.59	0.52	13000	4.5	94	0.0
025817.87+010946.0 ^{dfg}	18.15	-0.12	0.06	0.68	0.65	28000	3.5	110	2.8
030302.44–062829.9 ^g	19.77	0.44	0.13	0.61	0.63	15000	4.5	134	1.4
030544.41–074941.2	18.31	0.36	0.19	0.83	0.62	15000	5	69	6.4
030607.19–003114.4 ^{fg}	16.39	0.29	0.20	0.82	0.60	15000	5	32	9.3
030859.87–002735.8	19.64	0.75	0.73	1.06	0.64	9500	4.5	75	8.7
032136.55–001630.5 ^g	17.62	-0.16	-0.12	0.61	0.55	22000	4.5	64	6.1
032422.38–000516.1 ^g	19.33	0.01	0.08	0.66	0.62	18000	4.5	126	10.5
032428.78–004613.8 ^g	19.30	0.09	0.38	0.43	0.03	32000	4	233	1.5
032758.16–002215.5 ^g	19.52	0.96	0.88	1.08	0.64	10500	4	82	0.9
032842.92+001749.8 ^g	18.05	0.94	0.92	0.98	0.58	11000	2.5	46	0.0
033548.59+003832.3 ^{dg}	18.02	0.23	0.10	0.82	0.65	17000	4.5	62	0.0
034831.09–061400.5 ^g	19.63	0.33	0.01	0.65	0.60	15000	4.5	114	0.0
042328.12–003801.5	19.56	0.05	0.33	0.95	0.66	8000	3.5	43	27.0
074011.18+385909.1	19.06	0.32	-0.16	0.07	0.33	12000	6	80	0.0
074301.93+410655.3 ^f	17.32	0.14	-0.14	0.47	0.58	16000	5.5	43	3.1
074730.57+430403.6 ^f	18.75	0.50	0.41	0.92	0.75	9500	3	51	5.4
075009.90+381641.6	18.23	0.18	-0.09	0.57	0.56	11500	5	47	4.0
075223.15+433212.2	19.12	0.34	0.57	0.70	0.51	24000	4.5	158	5.3
083808.00+530254.4	19.39	-0.07	0.43	0.61	0.54	24000	2.5	40	4.4
084833.60+005840.0	18.78	0.30	0.26	0.91	0.67	12000	5	70	2.5
090925.42+533700.7	17.37	0.11	-0.01	0.57	0.56	17000	4	51	2.7
091849.56+545601.8	18.25	0.20	0.66	0.60	0.41	8000	1	26	0.4

Table 1—Continued

SDSS J	<i>g</i>	<i>u-g</i>	<i>g-r</i>	<i>r-i</i>	<i>i-z</i>	T(WD) ^a	M sp type ^b	d(pc) ^c	EW[H α]
103743.61+655448.0	18.36	0.38	-0.07	0.36	0.52	15000	6	63	14.8
104517.78-001833.7 ^g	18.33	0.14	-0.17	0.53	0.65	15000	5	65	0.7
105853.59+005608.6 ^g	18.93	0.11	0.33	0.37	0.28	19000	0	109	0.0
112307.36+003216.1	19.42	0.19	-0.13	0.62	0.58	15000	6	112	3.9
112357.73-011027.5	18.30	0.10	-0.28	0.13	0.50	15000	6.5	68	0.0
112623.88+010856.9 ^g	18.71	0.42	0.49	0.87	0.54	9500	3	46	3.5
112748.27-002859.9 ^g	18.34	0.37	-0.21	0.39	0.60	17000	5.5	78	0.8
112909.50+663704.4 ^f	17.70	0.26	-0.05	0.54	0.66	17000	4.5	62	12.4
113457.72+655408.7	18.24	0.02	0.07	0.58	0.54	12500	6	59	4.5
113722.25+014858.6 ^h	18.74	-0.08	0.15	0.38	0.59	42000	2.5	182	100.0
113800.35-001144.5 ^{dg}	18.82	0.30	-0.04	0.71	0.64	26000	5	135	0.0
114312.57+000926.5 ^{dg}	18.13	0.23	-0.11	0.51	0.65	16000	4.5	62	3.2
115156.94-000725.5 ^g	18.11	0.46	-0.03	0.33	0.51	10500	6.5	41	11.0
120507.97+031234.4	18.47	0.38	-0.05	0.46	0.65	12000	5	57	0.0
121033.77-004644.4 ^{dg}	18.92	0.24	0.53	1.11	0.67	8000	4	40	0.0
122339.62-005631.2 ^g	17.98	0.51	-0.16	0.15	0.34	13500	5.5	47	0.6
123922.34+005548.8 ^{dg}	19.24	0.27	0.03	0.83	0.67	16000	4.5	110	5.7
125207.17+012156.8	18.78	-0.03	0.28	0.58	0.41	9000	3	41	0.0
125250.03-020608.2	19.21	0.12	0.23	0.61	0.53	22000	1.5	158	0.0
132312.65-025456.1	18.02	0.33	0.59	1.09	0.69	8000	3.5	29	0.0
133953.89+015614.9	19.34	0.31	0.13	0.59	0.54	10500	3	71	6.9
140723.04+003841.8 ^d	17.66	0.04	-0.09	0.74	0.60	24000	4	76	3.7
141220.70+654123.3	19.17	0.35	-0.11	0.43	0.48	13000	5	84	2.0
141731.25+015059.0	18.71	0.37	0.02	0.60	0.54	13500	4.5	69	9.8
143947.62-010606.9 ^f	16.55	-0.36	-0.27	-0.01	0.11	40000	0	73	10.7
144258.48+001031.5 ^f	18.29	-0.01	0.03	0.78	0.72	32000	4.5	132	4.5
145300.99+005557.1 ^d	19.16	0.41	0.04	0.61	0.57	13000	5	80	2.0
145527.72+611504.8	19.24	0.03	-0.01	0.66	0.54	12500	5	94	0.0
150118.41+042232.3	19.58	-0.05	-0.01	0.48	0.51	16000	5.5	133	4.6
150231.66+011045.9 ^e	18.48	0.41	-0.03	0.43	0.56	13000	4	60	0.0
150648.12+002716.4	19.05	0.24	0.53	0.73	0.49	8500	3	41	9.0
151058.76+004112.7	19.39	0.45	-0.05	0.36	0.64	18000	6	125	16.0
152717.25+002413.4 ^g	19.60	0.55	-0.04	0.63	0.61	10000	6.5	61	0.0
152933.26+002031.2 ^{dg}	18.18	0.46	-0.15	0.34	0.53	16000	5.5	62	15.3
154219.45+032311.0	19.46	0.34	0.34	0.98	0.59	10500	3.5	76	0.0
155554.25+545417.4	18.86	-0.09	0.03	0.54	0.42	20000	2.5	116	0.0
161033.87+491536.7	18.77	0.04	-0.05	0.48	0.46	19000	3.5	99	0.0
161145.89+010327.8	18.76	0.77	0.09	0.59	0.67	20000	5	96	9.1
164615.60+422349.3	18.43	0.31	-0.13	0.59	0.75	15000	6.5	74	16.6
165005.16+390426.4 ^g	18.73	-0.06	-0.15	0.55	0.55	15000	5.5	91	9.0
170459.71+384433.0	18.34	0.18	-0.04	0.47	0.49	19000	4	77	0.0
171145.43+555444.5 ^{dg}	18.24	-0.32	-0.34	0.32	0.51	32000	4.5	130	1.5

Table 1—Continued

SDSS J	<i>g</i>	<i>u-g</i>	<i>g-r</i>	<i>r-i</i>	<i>i-z</i>	T(WD) ^a	M sp type ^b	d(pc) ^c	EW[H α]
172601.55+560527.1 ^{dg}	19.20	0.22	0.30	0.76	0.49	16000	3.5	101	4.4
172715.57+542938.1 ^g	19.37	0.47	0.47	0.87	0.55	11500	3.5	86	4.5
172831.84+620426.5 ^g	18.80	0.34	0.59	0.89	0.60	16000	5	72	14.0
173101.49+623316.0 ^g	18.18	0.31	-0.12	0.57	0.65	17000	5.5	118	0.0
214720.96+130227.4	19.62	0.06	0.03	0.52	0.52	17000	4	147	0.0
221714.49+004601.3	19.42	0.36	0.10	0.60	0.71	17000	5.5	113	0.0
231221.60+010127.0	18.66	0.19	0.61	1.02	0.66	20000	3.5	128	0.0
231230.79+005321.7 ^f	17.23	0.13	0.53	0.71	0.51	22000	3	64	8.8
233919.65–000233.8	19.14	0.91	0.74	0.92	0.58	9000	3.5	53	0.0
234459.62+002750.0	19.42	0.40	-0.13	1.82	0.94	8000	5.5	52	5.0
234649.94–002032.2	18.15	0.27	0.30	0.64	0.36	9500	2.5	30	3.0

^aWhite Dwarf Primary Temperature (K): Errors are $\pm 2000\text{K}$ for $T \leq 20,000\text{K}$, $\pm 4000\text{K}$ for $T > 20,000\text{K}$

^bSecondary M Spectral Type: Errors are $\pm 1-2$ subclasses

^cDistance errors are $\pm 20\%$

^dThese objects have been observed twice by SDSS

^eThis object has been observed three times by SDSS

^fThese objects have followup APO observations. See Table 3.

^gThese objects are in the SDSS Early Data Release (EDR). See Stoughton et al 2002.

^hThis object is a CV discovered by our photometric search pipeline.

Table 2. M Dwarf Secondary Magnetic Activity Data

M spectral type	Objects ^a	Active Objects ^b	Log[Mean($L_{H\alpha}/L_{bol}$)] ^c	Error(dex) ^d
0	2	0	–	–
0.5	0	0	–	–
1	1	1	-4.29	0.76
1.5	1	0	–	–
2	2	0	–	–
2.5	8	6	-3.02	0.08
3	11	9	-2.61	0.21
3.5	9	7	-2.76	0.10
4	12	8	-2.47	0.44
4.5	16	9	-3.33	0.33
5	22	10	-3.49	0.36
5.5	13	9	-3.77	0.62
6	6	4	-4.98	2.08
6.5	4	1	-4.11	1.74
7	2	0	–	–

^aNumber of Objects in spectral type bin.

^bNumber of Objects in spectral type bin which are magnetically active.

^cMean activity level of the active objects in each spectral type bin.

^dError in the logarithm of the mean $L_{H\alpha}/L_{bol}$ for each spectral type bin.

Table 3. APO Followup Data^a

SDSS J	Nspec ^b	Hours ^c	Dates ^d	V_{min} ^e	Comments
001749.25–000955.4	3	–	E,F	27	very blue SED
023515.12–000737.0	3	–	E,F	32	
025817.87+010946.0	3	–	E,F	14	
030607.19–003114.4	12	2	A,E,F	320	
074301.93+410655.3	3	–	G	23	
074730.57+430403.7	19	4	B,E,G,H	250	
075223.15+433212.2	5	–	E,G,H	96	
112909.50+663704.4	17	3	B,C,G	137	4.1 hour period
143947.62–010606.9	25	5.5	C	91	
144258.48–001031.5	2	–	B,D	150	
172441.80+593103.3	9	2.5	C	59	
231230.79+005321.7	3	–	D,F	27	

^aFinding charts were obtained from the STScI Digitized Sky Survey at http://archive.stsci.edu/cgi-bin/dss_form

^bNumber of APO spectra taken

^cHours of continuous observation on a single night

^dDates of APO spectra taken: A=9/13/2000, B=4/15/2001, C=5/4/2001, D=6/17/2001, E=10/15/2001, F=12/7/2001, G=12/18/2001, H=12/19/2001

^eMinimum radial velocity variation in km s^{-1} , derived from the maximum wavelength variation in the $\text{H}\alpha$ emission line.